

Response to low-dose X-irradiation is p53-dependent in a papillary thyroid carcinoma model system

KHALIL ABOU-EL-ARDAT^{1,2*}, HANANE DERRADJI¹, WINNOK DE VOS², TIM DE MEYER²,
SOFIE BEKAERT², WIM VAN CRIEKINGE² and SARAH BAATOUT¹

¹Laboratory of Molecular and Cellular Biology, Radiobiology Unit, Belgian Nuclear Research Center (SCK-CEN), Boeretang 200, 2400 Mol; ²Department of Molecular Biotechnology, FBW, Ghent University, 9000 Ghent, Belgium

Received February 21, 2011; Accepted March 24, 2011

DOI: 10.3892/ijo.2011.1175

Abstract. The link between high doses of radiation and thyroid cancer has been well established in various studies, as opposed to the effects of low doses. In this study, we investigated the effects of low-dose X-ray irradiation in a papillary thyroid carcinoma model with wild-type and mutated p53. A low dose of 62.5 mGy was enough to cause an upregulation of p16 and a decrease in the number of TPC-1 cells in the S phase, but not in the number of BCPAP p53-mutant cells. At a dose of 0.5 Gy, visible signs of senescence appeared only in the TPC-1 cells. We conclude that low doses of X-rays are enough to cause a change in cell cycle distribution, possibly p53-dependent p16 activation, but no significant apoptosis. Senescence requires higher doses of X-irradiation via a mechanism involving both p16 and p21.

Introduction

The causal link between ionizing radiation, DNA damage, and adverse health effects have been well established at high doses (1). However, there is still debate over the biological consequences of the effects induced at lower doses, and consequently there are uncertainties as to what constitutes a 'low dose' and how safe low doses are. This uncertainty is compounded by the choice of method used for determining the effect of low doses. Currently a linear no-threshold (LNT) model is used to extrapolate the effects of low-dose exposure from those at high doses. However, the accuracy of this model at low doses (doses below 10 mGy) has been challenged (2). A recent study by Averbeck portrays scientific evidence against

the LNT model and comes to the conclusion that the LNT model may have to be abandoned as it does not describe what happens at low doses (3). Indeed, Rothkamm and Löbrich reported that there was a lack of DNA double-strand break (DSB) repair in fibroblasts irradiated with X-ray doses as low as 1 mGy (4). However, they did show that the detection of γ -H2AX foci is possible even at such low doses, thus making it a suitable method for the study of the biological effects of low doses of radiation. Furthermore, another study on the effects of low and very low doses of radiation on a human mesenchymal cell line at different time-points supports a non-linear model at low doses (5). Currently, low doses of radiation are commonly defined as anything between background radiation [\sim 0.01 millisievert (mSv)/day] and high doses of radiation (\geq 150 mSv/day) (6).

Studies on the effect of low-dose irradiation are non-trivial. After the Chernobyl nuclear disaster, large amounts of radioactive iodine isotopes were released into the atmosphere (7). The effect of the radioiodine became apparent in the early nineties, when increases in the frequency of thyroid cancer were reported in children from the countries surrounding the site (7,8). In addition, a high prevalence of RET/PTC3 rearrangement was reported in these patients (8). A link between external X-irradiation and thyroid tumor formation has already been reported by Christov in rats (9). Over a period of 18 months, the author noticed an increase in the incidence of thyroid tumors in rats irradiated once with 300 rads of X-rays. The potential for adverse health effects after low doses becomes crucial when taking into account that we are now more than 20 years away from the Chernobyl disaster. The danger of high-dose irradiation emitted is thus largely gone but the issue of the risks of exposure to low doses of radiation remains to be dealt with.

For the purpose of this study, a model system for papillary thyroid carcinoma (PTC) was exposed to a range of X-ray doses, ranging from what is considered a 'low dose' (0.0625 Gy) to high doses (0.25, 0.5, 1 and 4 Gy) and the changes in viability, necrosis, apoptosis, cellular morphology, and the cell cycle were monitored. The model system consisted of two different cell-lines, TPC-1 and BCPAP. TPC-1 is a PTC cell line of human origin which harbors a constitutive RET/PTC1 rearrangement while BCPAP is a cell line of the same origin but with a V600E BRAF mutation and a mutated copy of p53.

Correspondence to: Mr Khalil Abou-El-Ardat, SCK-CEN, Boeretang 200, 2400 Mol, Belgium
E-mail: kabouela@sckcen.be

Abbreviations: LNT, linear no-threshold; mSv, millisievert; Gy, gray; SA β -gal, senescence-associated β -galactosidase; SASP, senescence-associated secretory phenotype

Key words: papillary thyroid carcinoma, RET/PTC1, apoptosis, p53, p73, radiation

The RET/PTC and BRAF mutations were found to work on the same signaling axis and had a common gene signature (10). The main difference is therefore the p53 mutational status, which allows us to infer conclusions on the role of the p53 pathway in low- and high-dose X-irradiation. Furthermore, cell lines provide a more homogeneous model to work with, something which is important when working with low doses of radiation, where the effects could be subtle and easy to miss in a heterogeneous system.

Materials and methods

Cell culture. TPC-1 cells (kindly provided by Dr Horst Zitzelsberger, Helmholtz Zentrum München, GmbH, Munich, Germany), which are thyroid papillary carcinoma cells of human origin, were cultured in 25 cm²-tissue culture flasks in Dulbecco's Modified Essential Medium (Gibco Invitrogen, Paisley, UK) supplemented with 4 mM L-glutamine and 10% v/v fetal bovine serum (FBS) (Gibco Invitrogen) in a humidified incubator (37°C; 5% CO₂). BCPAP [provided by Dr Jacques Dumont, Université Libre du Bruxelles (ULB), Brussels, Belgium] were cultured in Roswell Park Memorial Institute (RPMI)-1640 supplemented with 10% FBS in a humidified incubator (37°C; 5% CO₂). No antibiotics were added to the culture medium. For all experiments the earliest possible passage of cells was used (p22 for TPC-1 and p7 for BCPAP). For experiments on supernatants in TPC-1 cells, three different passages were used one of which was p22. The cells were tested for mycoplasma contamination and were found to be contamination-free.

Cell irradiation. Cells were plated at an initial cell density of 1x10⁶ cells per flask 24 h prior to irradiation. The medium was replenished prior to irradiation. Cells were irradiated using 250 kV, 15 mA, 1 mm Cu-filtered X-rays (delivered at 5 mGy/sec from a Pentak HF420 RX machine). Doses used were 0.0625, 0.25, 0.5, 1, or 4 Gy, while non-exposed cultures were sham-irradiated using a procedure identical to the 4 Gy irradiation. Doses in Gy were calculated using the same criteria used in medical practice to calculate doses given to tissues (i.e. 95% of roentgen exposure). The cells were then returned to the humidified incubator until harvest.

Cell viability, counting and morphology. Cell viability was assessed using the trypan blue dye exclusion method, cell numbers by a Beckman Coulter EPICS XL-MCL and fluorescent microspheres at 24 and 48 h post-irradiation. A volume with a known amount of microspheres was mixed with a volume of PBS containing an unknown number of cells. The mixture was passed in a flow cytometer which counted 10,000 cells and a certain number of microspheres. Using the known concentration of microspheres, the number of microspheres counted and the number of cells, it was possible to calculate the initial concentration of cells. Cellular morphology was determined at 24 h post-irradiation by examining May-Grünwald Giemsa stained cells after centrifuging them onto glass microscope slides.

Cell cycle and Annexin V/propidium iodide (PI). Cell cycle stages were quantified by EPICS XL-MCL flow cytometric

analysis of PI-stained cells. Complications due to clumps or doublet cells were avoided by excluding the compromised region by gating. Apoptotic and necrotic cell numbers were ascertained with FITC-conjugated Annexin V antibody and PI staining (Bender MedSystems Diagnostics, GmbH, Vienna, Austria) according to the manufacturer's instructions.

Caspase-3 levels using flow cytometry. Irradiated TPC-1 cells were trypsinized and pelleted (1500 rpm for 5 min) and the manufacturer's instructions were followed:

For caspase-3: The CaspGLOW Fluorescein Active Caspase-3 Staining Kit (Medical & Biological Laboratories Co., Ltd., Woburn, MA, USA) was used according to the manufacturer's instructions. Briefly, a substrate that is cleaved by active caspase-3 to release fluorescence was added to 3.3x10⁵ TPC-1 cells and incubated for 1 h in a humidified incubator. The cells were pelleted and washed twice with PBS and then suspended in 1 ml of PBS and read by flow cytometry.

Western blotting. Irradiated cells were pelleted by centrifugation and washed with PBS before being pelleted and frozen at -80°C. On the day of the experiment, the pellet was thawed and proteins extracted using Ready Prep II (BioRad) and a cocktail of protease inhibitors and phenylmethylsulfonyl fluoride following the manufacturer's instructions. The proteins were quantified using Bradford solution (BioRad) on a spectrophotometer at 595 nm. Proteins (30 µg) were loaded onto a 10% polyacrylamide gel followed by electrophoresis. The bands were transferred electrophoretically onto a polyvinylidene difluoride membrane, the loading controlled using Ponceau S staining, and the membrane probed with primary monoclonal antibodies against p53 (53 kDa), p21 (21 kDa) (Sigma-Aldrich), p73 (73 kDa), Akt (56-60 kDa), Bcl-2 (26 kDa) and p16 (16 kDa) (Santa Cruz). For p16, an antibody that recognizes both the mutated and normal form of the protein was used as TPC-1 has been reported to harbor a mutated copy of the protein (11). Horseradish peroxidase-conjugated secondary antibodies were used and the bands were visualized on an X-ray film by chemiluminescence (Amersham ECL Western Analysis System; GE Healthcare, UK) and equal loading was verified using β-tubulin as the housekeeping protein.

TGF-β1 ELISA. Twenty-four hours after irradiation, TPC-1 and BCPAP cell supernatants were collected and frozen at -80°C until the day of the experiment. TGF-β1 was quantified using the human/mouse TGF-β1 ELISA Ready-SET-Go! Kit (eBioscience, Vienna, Austria) according to the manufacturer's instructions. In brief, the supernatants were thawed and activated using 1 N HCl for 10 min, after which the HCl was neutralized with 1 N NaOH. A 96-well ELISA plate was coated with an antibody against TGF-β1, the supernatants were loaded onto the plate in triplicates and incubated overnight in the plate at 4°C. The plate was then washed, probed with primary antibody against TGF-β1, washed again and probed with a secondary antibody against the primary one. A substrate buffer supplied with the kit was used to visualize the color and 1 M H₂SO₄ was used as the stop solution. The resultant yellow color, corresponding to levels of TGF-β1, was measured using a spectrophotometer at 450 nm. A standard curve for purified

TGF- β 1 was used to correlate the absorbance with the concentration of TGF- β 1.

Detection of γ -H2AX foci. Immunohistochemistry: TPC-1 cells were plated at 500,000 cells per coverslip and irradiated with various doses of X-rays. The cells were fixed with 4% paraformaldehyde 30 min after irradiation and probed overnight with a primary antibody against the phosphorylated form of the histone H2AX (γ -H2AX) (Abcam, Cambridge, UK) and subsequently with a FITC-linked secondary antibody against the primary one. The coverslips were mounted onto glass slides and the images were acquired using a wide-field Nikon TE2000E epifluorescence microscope (25 different frames/slide, 5 plains of depth of 1 μ m thickness). Images were analyzed using Image J software (Rasband, NIH, Bethesda, MA, USA) and nuclei and γ -H2AX spots along with their respective sizes were calculated as previously described (12) (algorithm kindly supplied by Dr W. de Vos, Ghent University, Ghent Belgium). In total, around 1,300 nuclei from four different coverslips were scored and the number of foci for each nucleus was reported by the algorithm. The algorithm also determined the average spot occupancy, the area of the nucleus occupied by one focus, as a means to determine the size of the foci independent of the cell cycle. The median number of foci per nucleus and spot occupancy and their interquartile range was calculated for each irradiation dose using Microsoft Excel and SPSS software.

Senescence-associated (SA) β -galactosidase (SA β -gal) quantification by fluorescence. Cells were plated and irradiated with various doses of X-rays. The amount of β -galactosidase was measured 24 h later by monitoring the conversion of a substrate to 4-methylumbelliferone (4-MU) at pH 6.0 (BetaFluor β -Galactosidase Assay Kit (Novagen, WI, USA) as mentioned in the study by Gary and Kindell (13). β -galactosidase was quantified using a fluorometer (Fluoroskan Ascent CF, Thermo Labsystems, Waltham, MA, USA) with excitation at 360 nm and emission at 440 nm. A flask of cells was kept at confluence for comparison. This method allowed for a more quantitative approach to the β -galactosidase level measurement.

Cytokine level measurement using multiplex bead assay. Supernatants collected from both irradiation and sham-irradiated TPC-1 cells were incubated in a 96-well plate with dye-injected synthetic beads conjugated with antibodies against 90 different cytokines (Millipore Co., MA, USA). Each bead has a certain signature which helps to identify the associated cytokine. The cytokines were targeted with fluorescence-conjugated primary antibodies against that cytokine. The beads were passed through two intersecting lasers in a Luminex 100 instrument, one to excite the beads and the other to excite the probe. The beads were sorted automatically and the average fluorescence was reported for each well.

Statistical analysis. All experiments were carried out in biological triplicates except for the immunostaining experiments. The Dunnett test, a post-hoc test for multiple comparisons between irradiated and control conditions, was used to

compare experimental samples to the control using the SPSS software package version 11.5. For the ELISA experiment, a univariate analysis of variance (ANOVA) was performed with passage and radiation dose effect as factors. For γ -H2AX foci scoring, the Mann-Whitney test and the Kruskal-Wallis mean rank test were used with a post-hoc modification for multiple comparisons. Results were considered significant at $p < 0.05$. Boxplots were created using SPSS software while all other graphs were created using GraphPad Prism software version 5.00 (GraphPad Software Inc., La Jolla, CA, USA).

Results

All the experiments described below were performed on TPC-1 cells. As the results indicated a role for the p53 pathway, several experiments were repeated on BCPAP cells to investigate the latter hypothesis.

Irradiation causes an increase in amount of DSBs in TPC-1 cells. To investigate the level of DNA damage upon radiation of TPC-1 cells with various doses of X-rays, we quantified the amount of DNA DSBs using a microscopic analysis 30 min after irradiation. This method not only provides a sensitive method for detecting DNA damage foci but also allows for an analysis of their size. Calculation of the foci size was done using a parameter known as spot occupancy which measures the percentage of the nucleus occupied by the foci and adjusts for cell cycle variations and spot segmentation problems (14). Irradiation at a dose of 62.5 mGy caused a slight increase in the percentage of nuclei with observable DNA damage from around 1% in the control cells to 8% (Fig. 1; $p < 0.05$). At a dose of 4 Gy, the percentage of nuclei with foci greatly increased to around 99%. However, there was no increase in the median number of foci per nucleus at the lowest irradiation dose compared to the control: 0 (0-0) vs. 0 (0-0) foci/nucleus [median (interquartile range)]. Only at the higher doses was there an increase to 2 (0-9) for 0.5 Gy, and 26 (19-32) foci per nucleus for 4 Gy (Fig. 2A), both significant at $p < 0.05$. The size of the foci as measured by spot occupancy also increased in a dose-dependent manner in cells irradiated with 0.5 and 4 Gy compared to the control ($p < 0.05$). However, for the low dose of 62.5 mGy, the size of the foci did not increase compared to the control (Fig. 2B).

As an increase in DNA damage usually leads to a halt in cell proliferation, we evaluated whether these dose-dependent effects also affected cells.

Irradiation causes a decrease in number of TPC-1 cells. The two cell counting methods used (trypan blue counting and fluorescent microfluorospheres) yielded consistent results (Spearman correlation $R = 0.861$). Low doses of X-irradiation of TPC-1 cells did not cause any significant change in the number of cells, while higher doses caused a significant decline (Fig. 3), both at 24 and 48 h. After irradiation at 4 Gy, half the number of cells was present in the cultures 24 h after irradiation and around 40% at 48 h compared to the relevant sham-irradiated control cultures. This indicates a possible increase in cell death or a decrease in proliferation (cell cycle arrest) in these cells upon irradiation, the scope of the following two paragraphs.

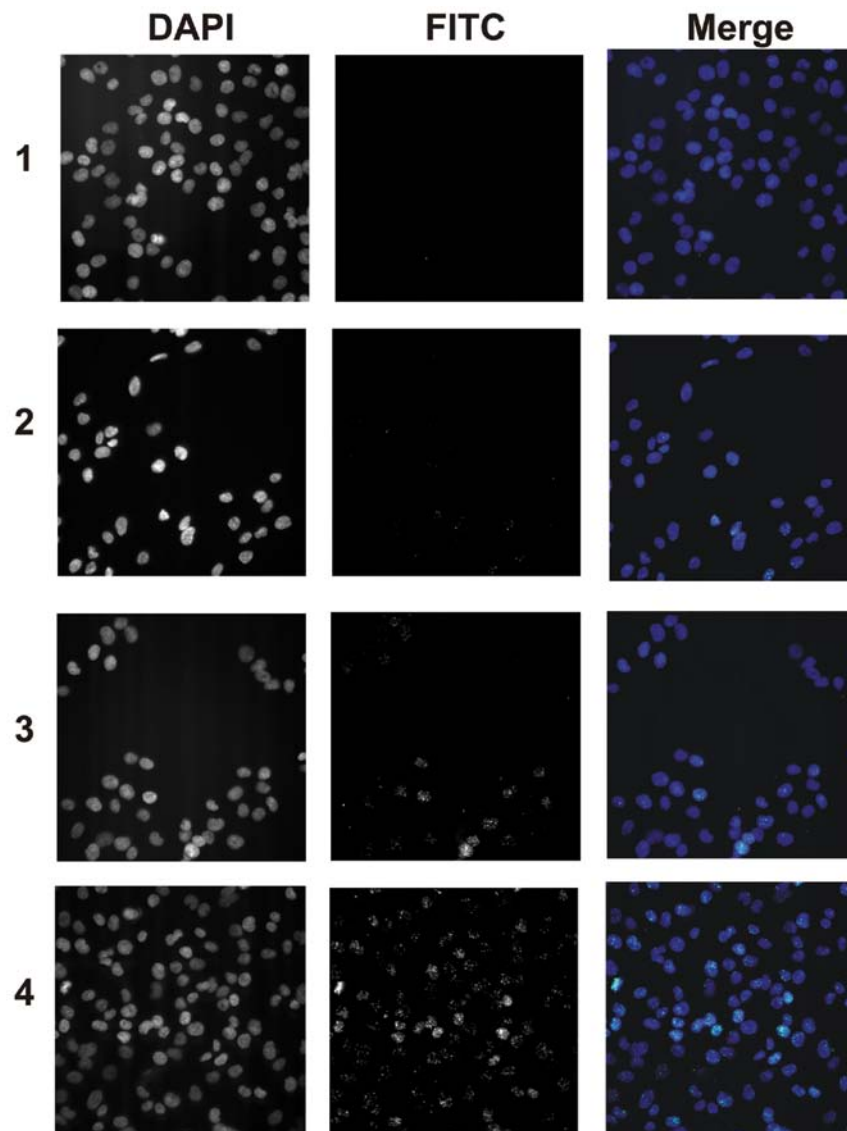


Figure 1. DNA DSB detection using γ -H2AX immunostaining. Images of TPC-1 cells taken using a wide-field Nikon TE2000E epifluorescence microscope fitted with a x40 objective lens. DNA damage foci were visualized by staining for γ -H2AX (FITC) while nuclei were stained with DAPI. Rows 1 to 4 are in the following order: Control, low (62.5 mGy), medium (0.5 Gy) and high (4 Gy) doses of X-rays. The merge column represents the DAPI (blue) and FITC (green) channels.

Cell cycle analysis using PI staining of DNA. To investigate the effect of X-rays on the cell cycle, we analyzed PI-treated cells with flow cytometry. At 24 and 48 h post-irradiation there was a dose-dependent decline in the number of S phase cells in TPC-1. This decline was significant at all doses even for the lowest (62.5 mGy) at 24 h, and reached a maximum of 75% at the highest irradiation dose (4 Gy) at 24 h and 83% at 48 h. These results indicate the possible activation of the G1/S and/or G2/M checkpoints in TPC-1 cells upon irradiation which is directly proportional to the irradiation dose. The cell distributions at 24 h post-irradiation are depicted in Fig. 4. The percentage of cells in each cell cycle phase is detailed in Table I.

To compare the effect that p53 plays in the cell cycle response, we performed the same experiment on BCPAP cells which are known to harbor a mutated copy of p53 (11). As in the TPC-1 cells, a decline in the number of cells in the S phase of the cell cycle was observed, but only at 1 and 4 Gy. However,

Table I. Percentage of TPC-1 cells in each cell cycle phase.

Dose (Gy)	G1	S	G2
0	67.27 \pm 0.99	9.52 \pm 0.51	15.39 \pm 0.75
0.0625	67.45 \pm 2.01	8.99 \pm 0.19	15.69 \pm 0.70
0.25	66.58 \pm 1.44	8.49 \pm 0.38	16.33 \pm 1.72
0.5	65.38 \pm 0.85	7.97 \pm 0.32	18.81 \pm 1.16
1	80.01 \pm 1.17	3.75 \pm 0.15	13.31 \pm 0.38
4	69.70 \pm 1.42	2.28 \pm 0.11	22.76 \pm 0.83

Numbers reported are: Percentage of cells (%) \pm SD.

there was a decline in G1 phase cells and an increase G2 phase cells. This indicates the possible activation of the G2/M checkpoint without G1/S checkpoint activation, which is not

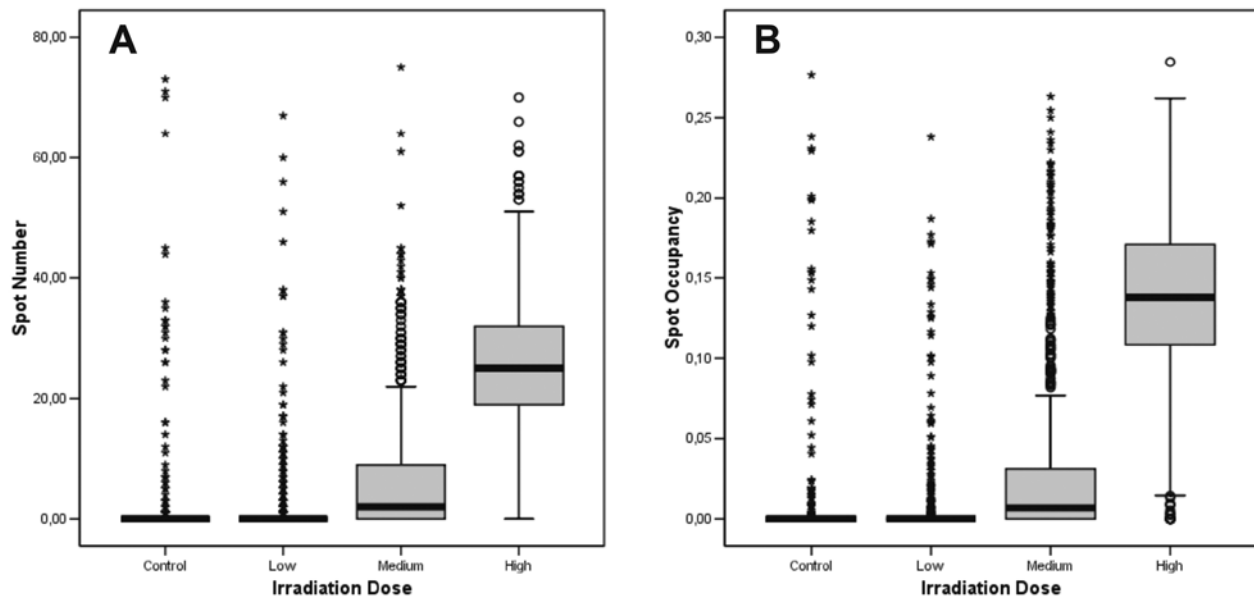


Figure 2. (A) Boxplot representing median spot number per nucleus vs. irradiation dose in TPC-1 cells 30 min post-irradiation. The box boundaries represent the upper and lower quartiles and the thick black line within represents the median. The whiskers represent the 95% confidence interval (CI) while the circles represent outliers and the asterisks extreme cases. An algorithm on Image J software was used to count the number of nuclei and foci in each nucleus. In total, around 1,300 nuclei were scored from four different coverslips and the median of foci per nucleus was calculated. Low, 62.5 mGy; medium, 0.5 Gy; and high, 4 Gy. Only medium and high doses are significant ($p < 0.05$). (B) Boxplot representing spot occupancy vs. irradiation dose in TPC-1 cells 30 min post-irradiation. The box boundaries represent the upper and lower quartiles and the thick black line within represents the median. The whiskers represent the 95% CI while the circles represent outliers and the asterisks extreme cases. Spot occupancy is used here as a more robust measure of spot size and was calculated using an algorithm on Image J software. Average occupancy was calculated for each nucleus and the median was calculated. Asterisks represent outliers. Low, 62.5 mGy; medium, 0.5 Gy; and high, 4 Gy. Only medium and high doses are significant.

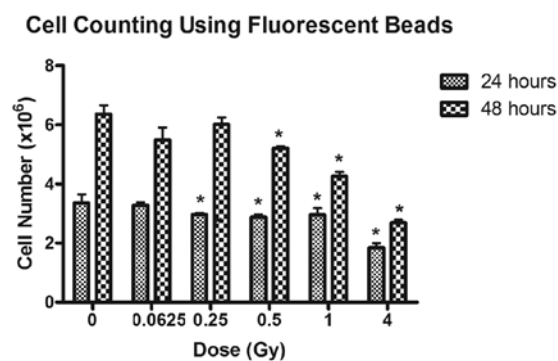


Figure 3. Cell number vs. irradiation dose in TPC-1 cells at 24 and 48 h post-irradiation. Histogram showing the number of cells (in millions) 24 and 48 h after irradiation with various doses of X-rays as measured by counting fluorescent beads alongside TPC-1 cells in a flow cytometer. Error bars represent the means \pm SD. Asterisks indicate significant results compared to the control at $p < 0.05$.

unexpected in cells with a mutant copy of p53 (15) (Fig. 4). The percentage of cells in each cell cycle phase is detailed in Table II.

Analysis of cell death induced by irradiation. To distinguish between apoptosis and necrosis, Annexin-V/PI staining was employed. A slight decline in the number of viable cells and an increase in apoptosis was observed. However, it was observed that, at 24 h post-irradiation, the predominant mode of death

Table II. Percentage of BCPAP cells in each cell cycle phase.

Dose (Gy)	G1	S	G2
0	82.34 \pm 1.89	5.77 \pm 0.49	11.09 \pm 1.30
0.0625	82.54 \pm 2.00	6.52 \pm 1.28	10.41 \pm 0.63
0.25	79.46 \pm 3.33	6.58 \pm 1.16	13.42 \pm 3.79
0.5	79.56 \pm 1.82	5.16 \pm 0.81	14.76 \pm 1.24
1	82.71 \pm 1.13	3.73 \pm 0.74	13.21 \pm 1.31
4	69.74 \pm 1.84	2.53 \pm 0.60	27.41 \pm 2.09

Numbers are reported as: Percentage of cells (%) \pm SD.

was necrosis at all irradiation doses. This was also the case at 48 h, except for the highest dose (4 Gy) where apoptosis became the most predominant mode.

To check whether apoptosis was further activated at later time-points in response to irradiation, Annexin V/PI double staining was also carried out on cells irradiated with X-rays after 72 h. In comparison to the control, TPC-1 cells 72 h post-irradiation displayed an increase in basal levels of Annexin-V-positive cells. This could be attributed to the fact that the cells had been in culture for >72 h without medium replenishment. However, apoptosis was not significant in comparison to the control except again, at the highest dose of irradiation (4 Gy). At the same dose, there was an increase in

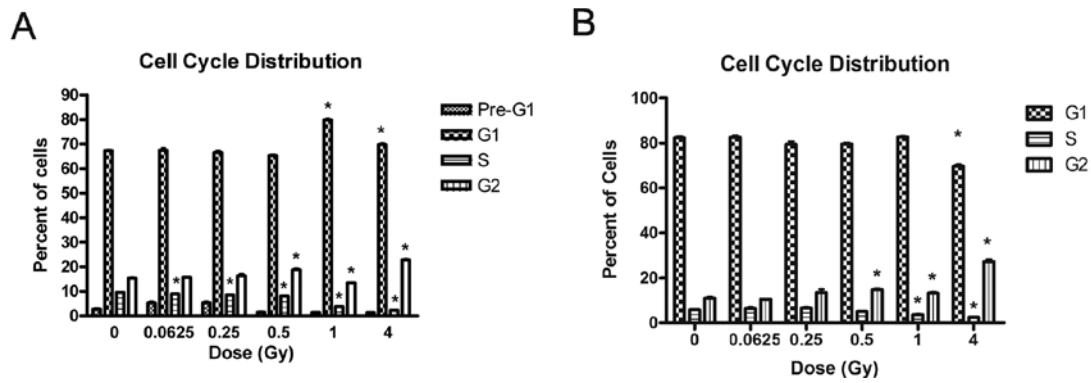


Figure 4. Cell cycle distribution by PI staining: Bar graph representing the percentage of cells in pre-G1, G1, S and G2. (A) TPC-1 cells and (B) BCPAP cells. Bars represent an average of 3 measurements. Error bars represent the means \pm SD. Asterisks represent significant results at $p < 0.05$.

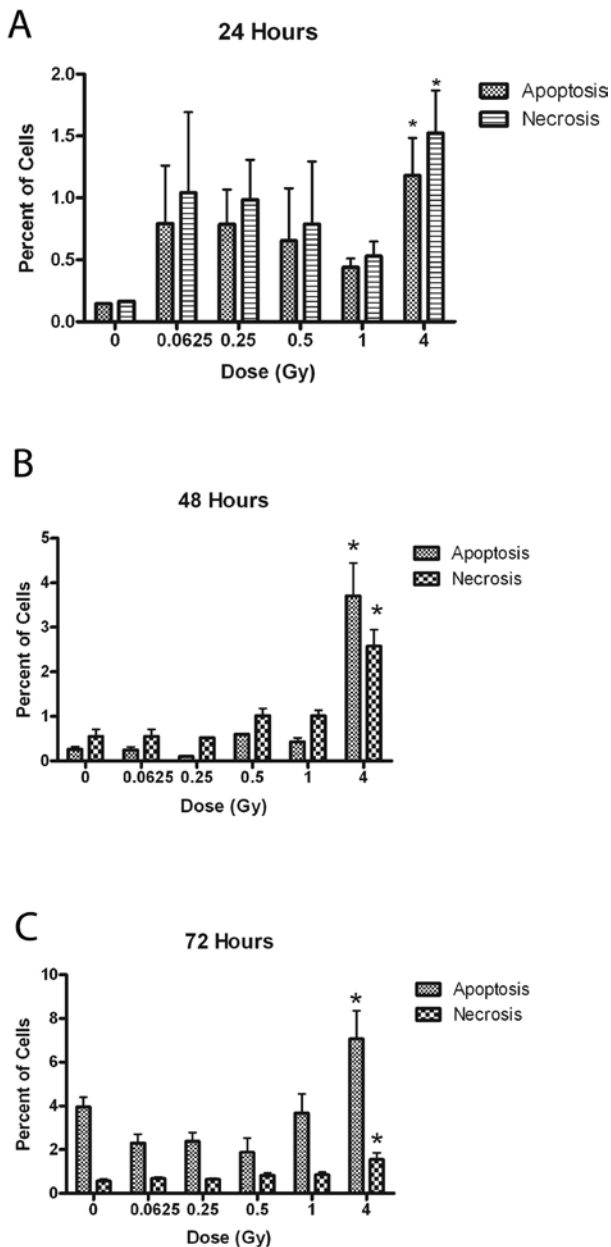


Figure 5. Apoptosis measurement using Annexin V/PI double staining. Bar graphs representing the percentage of apoptotic and necrotic cells (A) 24 h, (B) 48 h and (C) 72 h post irradiation in TPC-1 cells. Apoptotic cells were taken as Annexin V-positive/PI-negative and -positive cells whereas necrotic cells were taken as Annexin V-negative/PI-positive cells. Results reported as the percentage of cells \pm SD. Asterisks represent significant results at $p < 0.05$.

necrotic cells as well. At all time-points, irradiation at low doses did not increase apoptosis or necrosis significantly (Fig. 5A-C). However, the levels of apoptosis as measured by Annexin V/PI double staining did not increase in BCPAP cells 24 h post irradiation (data not shown).

Levels of caspase-3 after irradiation. The increase in the levels of apoptosis at the later time-points at 4 Gy led us to examine whether this was also reflected in the terminal marker, caspase-3. Cleaved caspase-3 levels did not alter significantly at 24 h post-irradiation but at 48 h post-irradiation they exhibited a dose-dependent increase with a significant up-regulation at 1 and 4 Gy (Fig. 6A). However, levels of cleaved caspase-3 did not increase significantly in the BCPAP cell line neither at 24 nor 48 h post-irradiation (Fig. 6B).

Subsequently, we wanted to assess whether the significant effects of high-dose irradiation on TPC-1 cells also induced morphological alterations, particularly in comparison to the BCPAP cells.

Changes in cellular morphology following irradiation. Senescence can be brought on by several factors, including stress such as radiation and DNA damage (16). This state is defined by several morphological and molecular markers. We therefore performed microscopic observations of the control and irradiated TPC-1 cells (Fig. 7A). The morphology of TPC-1 cells following irradiation showed alterations typical of stress induction. There was a marked increase in intracellular vesicle trafficking, as shown by the increased number of vesicles in the cytoplasm of irradiated cells (Fig. 7B). Similarly, there was evidence of nuclear fragmentation in some cells at the higher doses of irradiation (4 Gy). In addition, cells appeared to be more flattened and larger in size especially at higher doses of irradiation (0.5 Gy and above) (Fig. 7B). This morphology has been associated with an increase in cellular senescence. The appearance of these phenomena increased in a manner proportional to the dose of irradiation received. However, when we observed the BCPAP cells (Fig. 8B) cells under the microscope, we did not observe an increase in cell size and flattening in these cells as observed in the TPC-1 cells (Fig. 8A and B).

We then wished to further investigate TPC-1 senescence, with a particular focus on the cytokines and chemokines

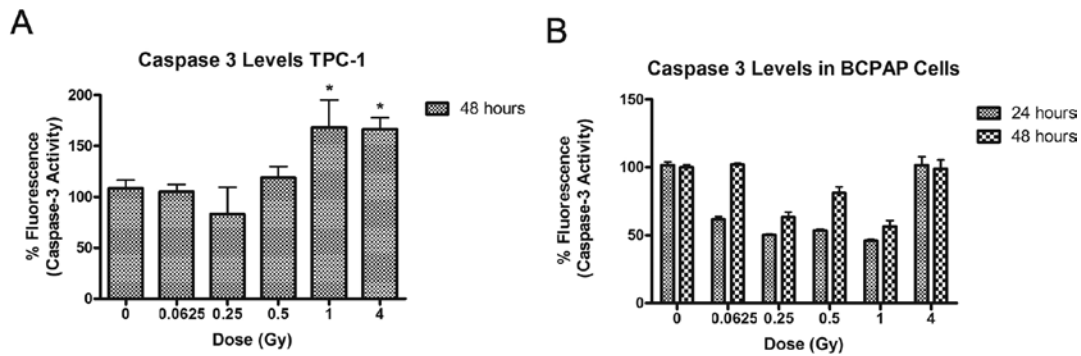


Figure 6. Caspase-3 levels in response to irradiation: Bar graphs displaying the levels of active caspase-3 in (A) TPC-1 and (B) BCPAP cells in response to various doses of X-irradiation. Results are reported as the percentage of fluorescence \pm SD. Asterisks represent significant results at $p < 0.05$.

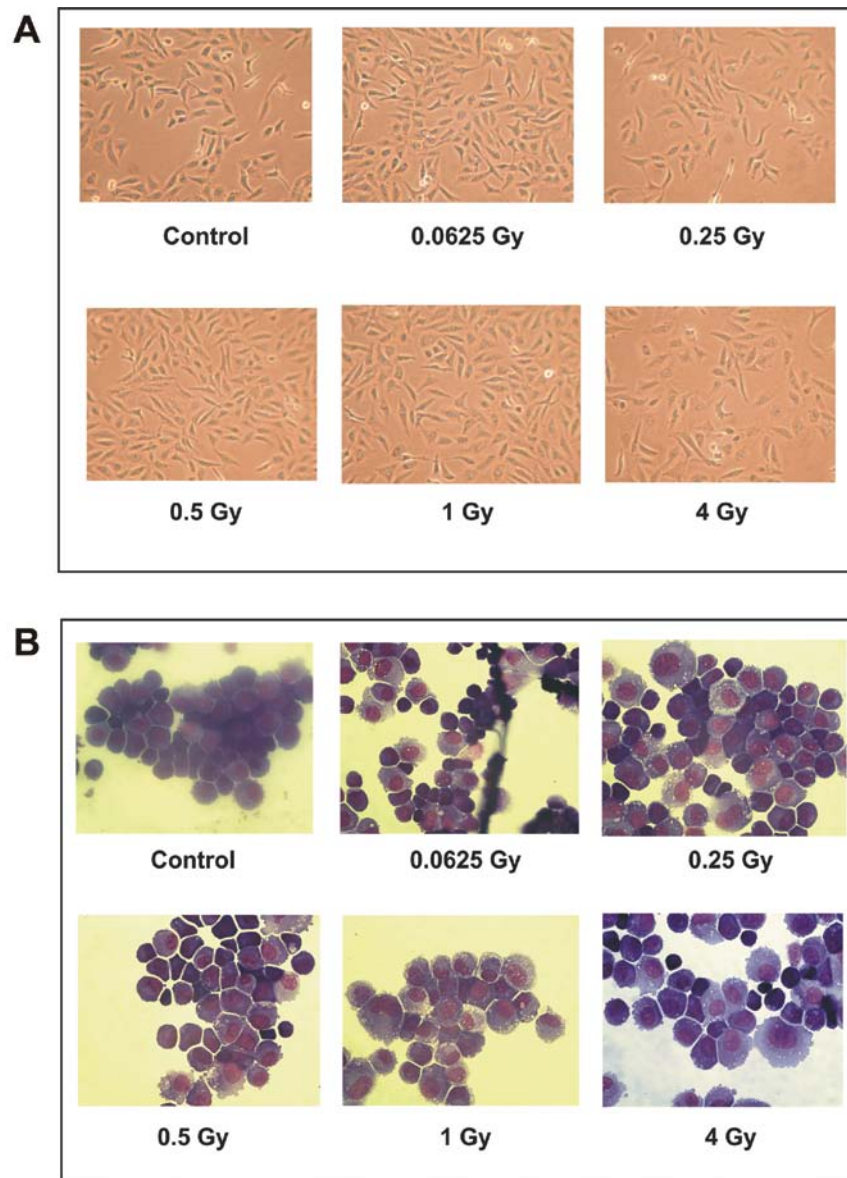


Figure 7. Morphological alterations in TPC-1 cells in response to radiation. (A) TPC-1 cells observed under an inverted light compound microscope (x60). (B) TPC-1 cells stained with the May-Grünwald Giemsa stain (x60).

involved. In the latter part of this study, we will further focus on the molecular differences possibly explaining the discrepancy in the TPC-1 and BCPAP response.

Effect of external X-irradiation on secreted levels of TGF- β 1. Senescent cells have been found to exhibit a distinct secretory profile, termed as senescence-associated secretory phenotype

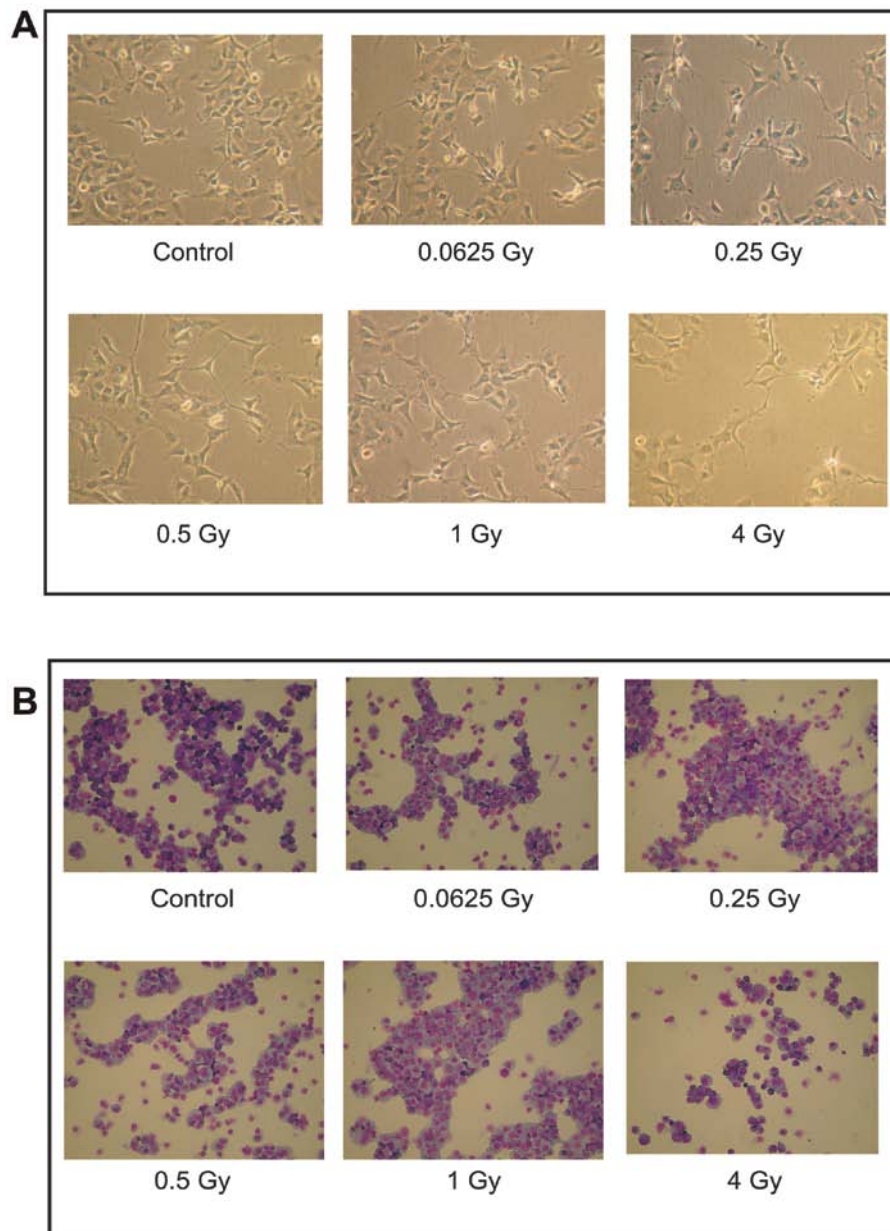


Figure 8. Morphological alterations in BCPAP cells in response to radiation. (A) BCPAP cells observed under an inverted light compound microscope (x60). (B) BCPAP cells stained with the May-Grünwald Giemsa stain (x40).

(SASP) (17). We therefore wished to investigate the milieu of TPC-1 cells for changes in secreted cytokines. A sandwich ELISA on the levels of TGF- β 1 was performed on the supernatant of TPC-1 cells collected 24 h after irradiation with various doses of X-rays. The supernatants were collected from cells of different passages and all supernatants were analyzed in a single 96-well plate. An analysis of TGF- β 1 levels with an adjustment for the passage number revealed that 0.5 Gy was the lowest significant dose to cause an up-regulation in the levels of TGF- β 1 (the Dunnett test; $p < 0.05$) (Fig. 9A). To confirm whether the lack of the morphological changes observed in the senescent cells would also mean no changes in the excreted levels of TGF- β 1, we performed a sandwich ELISA on the supernatant of BCPAP cells similar to the one performed on TPC-1 supernatants. There was no increase in the levels of TGF- β 1 in the case of BCPAP cells at all irradiation

doses. Indeed, there was a decrease in TGF- β 1 levels upon irradiation but when all three passages of cells were taken into account, this turned out not to be significant ($p < 0.05$) (Fig. 9B).

Effect of irradiation on the secreted level of cytokines using a multiplex bead assay. We further inspected the effect of radiation on a panel of cytokines and chemokines using a multiplex bead assay. We analyzed around 90 different cytokines and chemokines and came up with six significantly regulated factors whose regulation was affected by radiation. These factors included eotaxin, granulocyte macrophage colony stimulating factor (GM-CSF), interleukins (IL)-6 and -8, vascular endothelial growth factor (VEGF), and monocyte chemoattractant protein-1 (MCP-1). Eotaxin, GM-CSF, IL-8, and VEGF showed significant changes in their levels at only 4 Gy

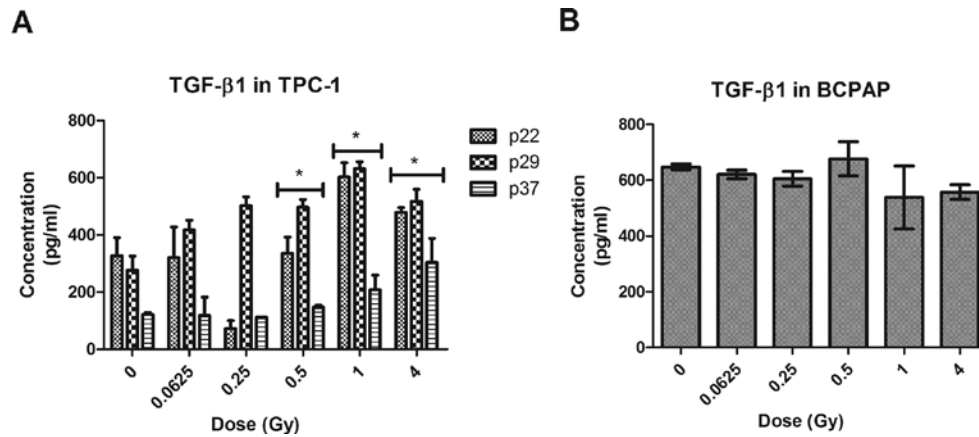


Figure 9. TGF-β1 levels in response to various doses of X-irradiation in TPC-1 and BCPAP cells. TGF-β1 concentrations (pg/ml) in the milieu of TPC-1 (A) and BCPAP (B) cells 24 h post-irradiation as measured by sandwich ELISA. Asterisks represent significant results at $p < 0.05$. An increase in the levels of TGF-β1 upon irradiation is evident at 0.5 Gy in TPC-1 cells but not in BCPAP. Error bars represent the means \pm SD.

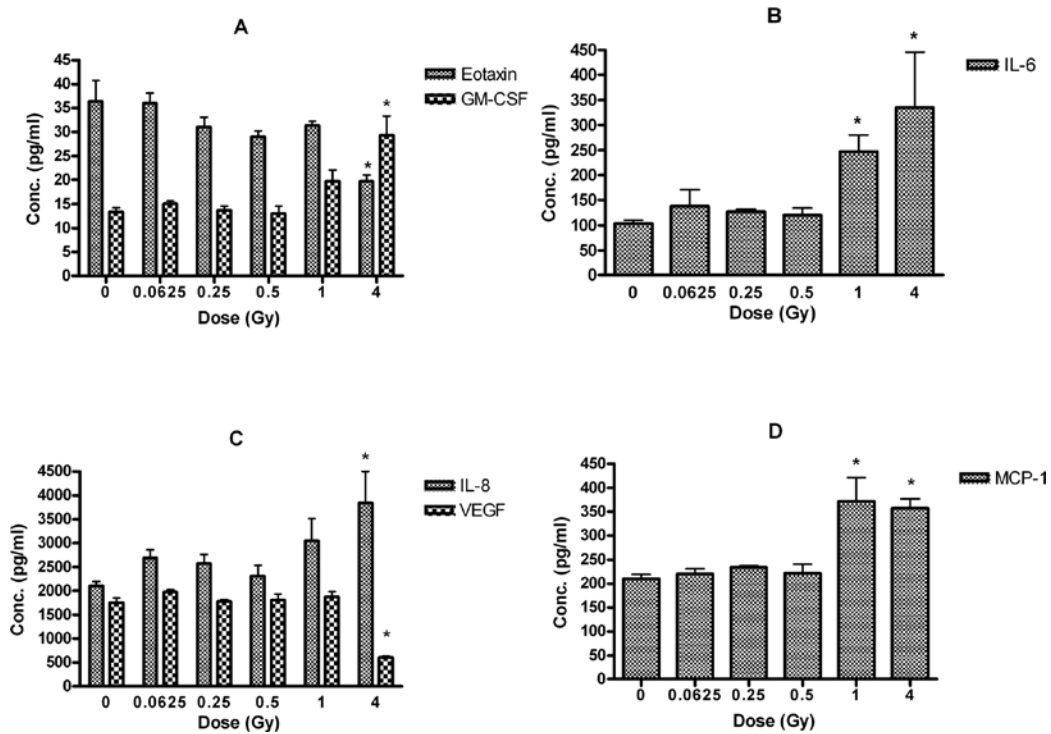


Figure 10. Concentration of secreted cytokines by multiplex bead assay. Measured concentrations (pg/ml) of various cytokines in the milieu of TPC-1 cells 24 h post-irradiation. (A) Eotaxin and GM-CSF, (B) IL-6, (C) IL-8 and VEGF and (D) MCP-1. Asterisks represent significant results at $p < 0.05$. Error bars represent the means \pm SD.

of X-rays. GM-CSF and IL-8 were up-regulated while VEGF and eotaxin were down-regulated. IL-6 and MCP-1 levels were significantly up-regulated at 1 and 4 Gy ($p < 0.05$) (Fig. 10).

Translational levels of molecular markers by Western blotting.

In order to gain insight into the molecular mechanisms underlying the differences in response to low and high doses of radiation in the two cell lines, we checked the levels of some of the central players in DNA damage response. A central player in the cellular DNA damage response is the tumor suppressor, p53 (18). As can be seen in Fig. 11A, p53 levels increased dose-dependently in the irradiated TPC-1

cells starting at a dose of 0.5 Gy. To further confirm that p53 was indeed active, the levels of one of its downstream targets, p21, were checked. Western blot analysis of p21 showed a dose-dependent up-regulation upon irradiation at doses of 0.5 Gy and above. This up-regulation was similar to that observed with p53. We also analyzed the response of another p53 family member, p73, to irradiation and found it to be absent in this cell line. To investigate the response of this cell line to apoptosis, the levels of two anti-apoptotic proteins, Bcl-2 and Akt, were assessed and were found to be up-regulated at all doses of radiation except 0.5 Gy (Fig. 11A and B). The lack of up-regulation at 0.5 Gy may point to the fact that Bcl-2 and Akt are not the only two anti-apoptotic

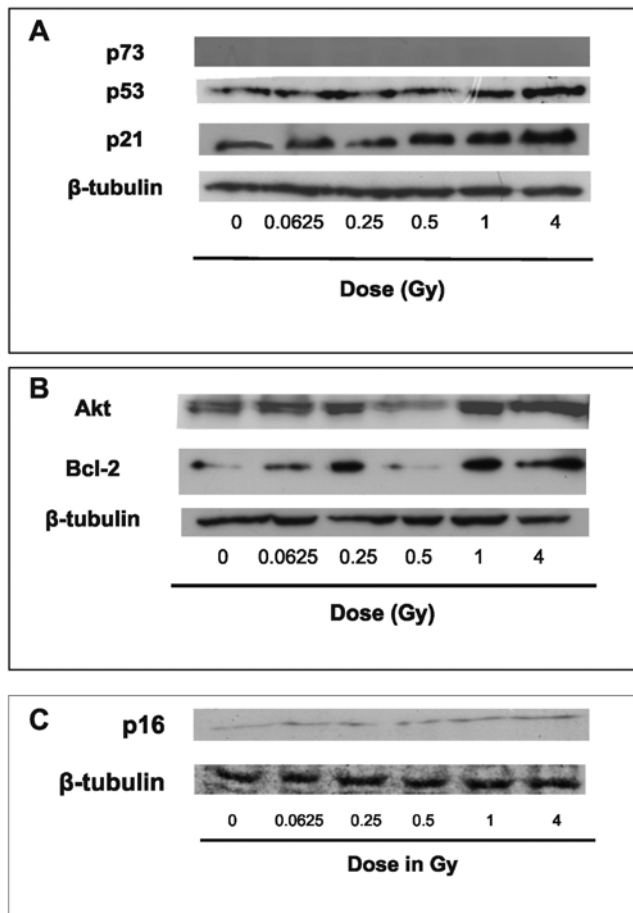


Figure 11. Response of various molecular markers to radiation in TPC-1 cells as measured by Western blot analysis. Translational levels of (A) the p53 family members, p73 and p53, and their downstream effector, p21, (B) the anti-apoptotic factors, Akt and Bcl-2, and (C) p16. β -tubulin was used as the housekeeping protein.

factors at play here and that there may be other players, such as Bcl-X_L.

As mentioned above, upon irradiation, cells presented signs of senescence, such as distinct morphological features, inhibition of proliferation, resistance to apoptosis and an altered secretory profile, and therefore, we checked the effect of radiation on p16^{INK4a} translational levels. As shown in Fig. 11C, radiation caused an increase in the levels of p16 in TPC-1 cells. The levels of p16 were up-regulated even at the low dose of irradiation (62.5 mGy) which warrants further research into the role of low doses of radiation in senescence.

To ascertain the effect of p53 on the induction of p16 and the senescence-like profile, we investigated the effect of a range of external X-rays on the levels of p16 and p73 in BCPAP cells. The tumor suppressor p53 was detected in BCPAP cells but upon irradiation the protein levels of p53 did not increase and neither did the levels of p73 and p16 (Fig. 12).

Effect of irradiation on levels of β -galactosidase. The increase in the levels of β -galactosidase measured at pH 6.0, (SA β -gal), is one of the hallmarks of senescence but not limited to it (19). To measure the levels of this enzyme in TPC-1 cells, we adapted a fluorescence assay and used various

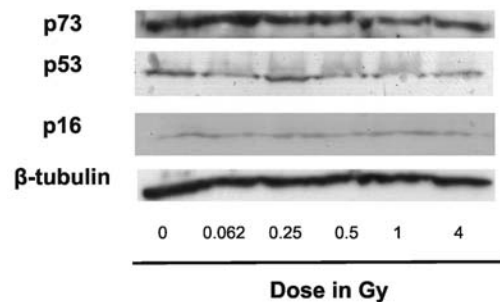


Figure 12. Response of various molecular markers to radiation in BCPAP cells as measured by Western blot analysis. Translational levels of p73, p53 and p16 in BCPAP cells. β -tubulin was used as the housekeeping protein.

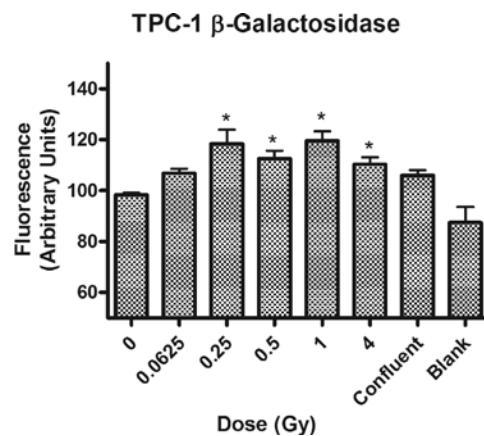


Figure 13. β -galactosidase level measurement in TPC-1 cells by fluorescence: Measured levels of SA β -galactosidase levels in TPC-1 cells 24 h post-irradiation. Confluent cells represent cells that were grown until fully covering the tissue culture flask bottoms while blank refers to cases with no cells. Asterisks represent significance at $p < 0.05$. Error bars represent the means \pm SD.

passages of TPC-1 cells as mentioned above. We noticed that fluorescence levels increased upon irradiation of TPC-1 cells starting at 0.25 Gy ($p < 0.05$). When cells were harvested until they formed a confluent monolayer, an increase in fluorescence was observed but was not significant when compared to the control ($p < 0.05$) (Fig. 13).

Discussion

Epidemiological evidence indicates a relationship between exposure to ionizing radiation and the induction of thyroid cancer, most notably following the study of children exposed to external irradiation and the victims of the Chernobyl disaster (20-22). In addition, Cardis *et al* (23) showed that there was a significant increase in the risk of certain cancers in workers of nuclear facilities (24). Radiation in the form of radioiodine is also used as a treatment for thyroid cancer albeit at higher doses (25), although studies have explored the possibility of using lower doses of radiation in cancer therapy for certain cancers (26-28). The risk of thyroid cancer from low-dose radiation exposures, such as those received from the environment, or from medical and workplace exposures, is uncertain.

We used a model system of two cell lines of PTC origin, one containing a wild-type copy of p53 and one with a

mutated copy and irradiated them with low (62.5 mGy) and moderate to high doses of X-rays (0.25, 0.5, 1 and 4 Gy) and monitored several parameters that were changed at various irradiation doses. This study shows that a low dose of radiation (62.5 mGy) elicits a response in cells with wild-type p53 (TPC-1) which differs from the response at higher doses. This could be mainly due to the difference in the molecular players involved. At the former dose, we observed a significant increase in the percentage of cells with DSBs, associated with a decrease in the fraction of cells in the S phase of the cell cycle and an up-regulation of p16 in TPC-1 cells, but not in BCPAP cells, thus indicating p53-dependency.

A decrease in the number of cells in the S phase and an increase in cells in the G2/M in TPC-1 cells at doses higher than 0.5 Gy was observed in our study at 24 and 48 h. This could be due to the fact that the TPC-1 cell line maintains a functional copy of p53. Although Frasca *et al* (29) sequenced the *TP53* gene in several PTC cell lines and found that TPC-1 harbored an inactivating K286E point mutation in p53, the study of Meireles *et al* has shown that TPC-1 carries wild-type p53 (11). Our results confirm the latter and point in the direction of TPC-1 having at least one functional copy of p53. Translational levels of p53 were up-regulated upon irradiation with X-ray doses of 0.5 Gy and above. p53 is known to activate the cyclin dependent kinase inhibitor (CDKN1A), p21, which is able to cause a G1/S checkpoint activation (30). Analyzing the levels of p21 revealed a similar increase in p21 levels upon X-ray doses of 0.5 Gy and above. A similar decrease in cells in the S phase was noted by Namba *et al* when they irradiated the NPA PTC cell line, at doses above 0.5 Gy and this was also found to be p53-dependent (31). Another member of the p53 family, p73, has also been found to be a tumor suppressor and to share the pathways that are associated with p53 (32,33). Therefore, p21 could feasibly be up-regulated by p73 and not by p53, and thus it warranted further investigation. By probing for p73, we found that there were no translational levels of this protein in TPC-1 cells. Frasca *et al* came to a similar conclusion when checking for transcriptional changes of p73 in TPC-1 cells by RT-PCR (29).

The up-regulation of p16 however, did not follow the same trend as p53 activation and could be responsible for the decrease of the fraction of cells in the S phase at the low dose of radiation. On the contrary, BCPAP, a cell line which harbors a mutant copy of p53, did not show any changes in the parameters measured at the low dose of irradiation. Evidence of cross-talk between the p53-p21 and p16-pRb pathways has existed for some time (34,35). However, the exact nature of this cross-talk is not entirely clear. It has now emerged that p53 may inhibit p16 levels and that in the absence of wild-type p53, p16 levels increase as a back-up mechanism (35,36). Our results suggest that the p16 response to radiation is dependent on the p53 status of the cells where the former was up-regulated in response to radiation in the TPC-1 cell line with wild-type p53. However, whether the one activates the other directly is not certain. Furthermore, the levels of p16 increased in response to various doses of X-rays despite the presence of a p53-mediated response. There was a decrease in the fraction of cells in the S phase only at 1 and 4 Gy and no increase in apoptosis as measured by the levels of active caspase-3 or the observed changes in morphology associated with senescence.

This was associated with no changes in the translational levels of p53, p73 and p16 in these cells upon external X-irradiation.

The up-regulation of p16 and p21 has been linked to the appearance of a senescence-like phenotype in cells. Senescence has been found to proceed via two interconnected pathways in which p53 and p16^{INK4a} lie at the center (16) and the appearance of a senescent profile has been mainly linked to the different dynamics of p21 and p16 where p21 is important for the appearance of the senescent profile while p16 maintains the cells in that state (37). The appearance of a senescent-like profile in the TPC-1 cells at 0.5 Gy and above and its absence at 62.5 mGy may point to the fact that the concomitant activation of both p21 and p16 and not only the latter is necessary for the appearance of this profile. These different dynamics in TPC-1 cells resemble those that were reported for melanocytes upon irradiation with different doses of UV (38). The difference in the appearance of a senescent-like profile between low and high doses of radiation is reflected in the increase in DNA DSBs in response to radiation. TPC-1 cells irradiated with a low dose of radiation (62.5 mGy) showed an increase in the percentage of nuclei displaying DNA damage with no change in the median number of foci or focus size. This is consistent with earlier reports indicating the absence of these phenomena below 0.1 Gy (39). At higher doses (0.5 and 4 Gy), the percentage of nuclei showing DNA damage, the median number and spot occupancy increased significantly compared to the control. More significantly, image analysis revealed a great increase in the size of the foci at 4 Gy. The size of the foci is indicative of the amount of DNA damage and the failure to repair the DNA damage caused the size of the foci to increase. Rodier *et al* (17) found that failure to repair DNA damage after 24 h at a dose of 10 Gy led to the appearance of large foci and was associated with a senescent profile.

The appearance of this senescent state at moderate to high doses of radiation would also explain the lack of apoptosis. The up-regulation of markers such as Bcl-2 and Akt could also explain the lack of apoptosis due to the reported role of these two molecules in the anti-apoptotic response (40,41). In fact, the up-regulation of Bcl-2 was found to push the cellular response to DNA damage from apoptotic to senescent (42). However, this does not explain the lack of apoptosis at lower doses of radiation especially since previous research has indicated that transformed cell lines of adenocarcinoma and glioma with a functional copy of p53 display low-dose hyper-radiosensitivity which is cell cycle- and apoptosis-dependent (43,44). Perhaps the low number of nuclei that exhibit DNA damage and the slight increase in the levels of Bcl-2 and Akt at low doses contribute to this effect. Another feature of senescent cells is an alteration in their secretory profile which has been reported at low doses of radiation (0.2 Gy) with noticeable effects on the microenvironment (45). This SASP has been deemed an important player in the tissue micro-environment and in the maintenance of the senescent state in cells (46,47). Our results point to an alteration of the secretory profile of TPC-1 cells only at doses of 0.5 Gy and higher. We identified six factors that were altered upon X-irradiation: TGF- β 1, VEGF, eotaxin, IL-6, IL-8 and MCP-1. TGF- β 1 was found to contribute to the inhibition of proliferation of TPC-1 cells through SMAD2/3 and the up-regulation of p21 (48).

IL-6 and -8 are of particular importance since they are involved in the inflammatory response and have been linked to the induction and maintenance of senescence and found to be the two most robustly expressed of the SASP panel (45,46). These factors among others have already been detected in the supernatant of stress-induced senescent cells (17,49).

In conclusion, our results indicate that cell lines of PTC origin respond to external X-irradiation with a change in their cell cycle distribution irrespective of their p53 status. However, only when a functional copy of p53 is present do the cells alter their cell cycle distribution in response to low doses of radiation, concomitant with p16 up-regulation and the up-regulation of certain anti-apoptotic markers. However, a senescent-like profile only appears in these cells at higher irradiation doses. Finally, it could be said that the response of the TPC-1 cells is dependent on the level of DNA damage brought on by irradiation. At a low dose of radiation, there is no increase in the number of DNA damage foci per nucleus and thus p16 up-regulation may cause a reversible cell cycle arrest until the DNA damage is fixed. At higher doses of radiation, DNA damage is more severe and p53, p21 and p16 are up-regulated and this leads to a non-reversible senescent-like profile.

Acknowledgements

The authors are grateful to Professor Michael Atkinson (Helmholtz Zentrum, Munich, Germany) for his critical review of the manuscript and for his continuous support. K.A.-E.-A. is supported by a doctoral SCK-CEN/Ghent University grant. This study was funded by the EU Euratom Program (GENRISK-T contract FIP6-2006-036495 on 'defining the genetic component of thyroid cancer risk at low doses' and the DoReMi NoE agreement 249689 on 'low dose research towards multidisciplinary integration').

References

- Little JB: Cellular, molecular, and carcinogenic effects of radiation. *Hematol Oncol Clin North Am* 7: 337-352, 1993.
- Hooker AM, Bhat M, Day TK, Lane JM, Swinburne SJ, Morley AA and Sykes PJ: The linear no-threshold model does not hold for low-dose ionizing radiation. *Radiat Res* 162: 447-452, 2004.
- Averbeck D: Does scientific evidence support a change from the LNT model for low-dose radiation risk extrapolation? *Health Phys* 97: 493-504, 2009.
- Rothkamm K and Löbrich M: Evidence for a lack of DNA double-strand break repair in human cells exposed to very low X-ray doses. *Proc Natl Acad Sci USA* 100: 5057-5062, 2003.
- Jin YW, Na YJ, Lee YJ, An S, Lee J, Jung M, Kim H, Nam S, Kim C, Yang K, Kim S, Kim W, Park WY, Yoo KY, Kim C and Kim J: Comprehensive analysis of time- and dose-dependent patterns of gene expression in a human mesenchymal stem cell line exposed to low-dose ionizing radiation. *Oncol Rep* 19: 135-144, 2008.
- Bonner WM: Low-dose radiation: thresholds, bystander effects, and adaptive responses. *Proc Natl Acad Sci USA* 100: 4973-4975, 2003.
- Cardis E, Howe G, Bebesko V, Bogdanova T, Bouville A, Carr Z, Chumak V, Davis S, Demidchik Y, Zvonova I, *et al*: Cancer consequences of the chernobyl accident: 20 years on. *J Radiol Prot* 26: 127-140, 2006.
- Hatch M, Ron E, Bouville A, Zablotska L and Howe G: The chernobyl disaster: cancer following the accident at the chernobyl nuclear power plant. *Epidemiol Rev* 27: 56-66, 2005.
- Christov K: Thyroid cell proliferation in rats and induction of tumors by X-rays. *Cancer Res* 35: 1256-1262, 1975.
- Melillo RM, Castellone MD, Guarino V, De Falco V, Cirafici AM, Salvatore G, Caiazzo F, Basolo F, Giannini R, Kruhoffer M, Orntoft T, Fusco A and Santoro M: The RET/PTC-RAS-BRAF linear signaling cascade mediates the motile and mitogenic phenotype of thyroid cancer cells. *J Clin Invest* 115: 1068-1081, 2005.
- Meireles AM, Preto A, Rocha AS, Rebocho AP, Mximo V, Pereira-Castro I, Moreira S, Feijão T, Botelho T, Marques R, Trovisco V, Cirnes L, Alves C, Velho S, Soares P and Sobrinho-Simões M: Molecular and genotypic characterization of human thyroid follicular cell carcinoma-derived cell lines. *Thyroid* 17: 707-715, 2007.
- De Vos WH, Van Neste L, Dieriks B, Joss GH and Van Oostveldt P: High content image cytometry in the context of subnuclear organization. *Cytometry A* 77: 64-75, 2010.
- Gary RK and Kindell SM: Quantitative assay of senescence-associated β -galactosidase activity in mammalian cell extracts. *Anal Biochem* 343: 329-334, 2005.
- Dieriks B, De Vos WH, Derradji H, Baatout S and Van Oostveldt P: Medium-mediated DNA repair response after ionizing radiation is correlated with the increase of specific cytokines in human fibroblasts. *Mutat Res* 687: 40-48, 2010.
- Bache M, Pigorsch S, Dunst J, Würfl P, Meye A, Bartel F, Schmidt H, Rath FW and Taubert H: Loss of G2/M arrest correlates with radiosensitization in two human sarcoma cell lines with mutant p53. *Int J Cancer* 96: 110-117, 2001.
- Cichowski K and Hahn WC: Unexpected pieces to the senescence puzzle. *Cell* 133: 958-961, 2008.
- Rodier F, Coppé JP, Patil CK, Hoejmakers WAM, Muñoz DP, Raza SR, Freund A, Campeau E, Davalos AR and Campisi J: Persistent DNA damage signalling triggers senescence-associated inflammatory cytokine secretion. *Nat Cell Biol* 11: 973-981, 2009.
- Sengupta S and Harris CC: p53: Traffic cop at the crossroads of DNA repair and recombination. *Nat Rev Mol Cell Biol* 6: 44-55, 2005.
- Severino J, Allen RG, Balin S, Balin A and Cristofalo VJ: Is beta-galactosidase staining a marker of senescence in vitro and in vivo? *Exp Cell Res* 257: 162-171, 2000.
- Boice JD Jr: Radiation-induced thyroid cancer - What's new? *J Natl Cancer Inst* 97: 703-705, 2005.
- Tucker MA, Jones PH, Boice JD, Jr., Robison LL, Stone BJ, Stovall M, Jenkin RD, Lubin JH, Baum ES, Siegel SE, Meadows AT, Hoover RN and Fraumeni JF Jr: Therapeutic radiation at a young age is linked to secondary thyroid cancer. *Cancer Res* 51: 2885-2888, 1991.
- Schneider AB, Ron E, Lubin J, Stovall M and Gierlowski TC: Dose-response relationships for radiation-induced thyroid cancer and thyroid nodules: evidence for the prolonged effects of radiation on the thyroid. *J Clin Endocrinol Metab* 77: 362-369, 1993.
- Cardis E, Vrijheid M, Blettner M, Gilbert E, Hakama M, Hill C, Howe G, Kaldor J, Muirhead CR, Schubauer-Berigan M, Yoshimura T, *et al*: Risk of cancer after low doses of ionising radiation: retrospective cohort study in 15 countries. *BMJ* 331: 77, 2005.
- Kesminiene A, Evrard AS, Ivanov VK, Malakhova IV, Kurtinaitis J, Stengrevics A, Tekkel M, Anspaugh LR, Bouville A, Chekin S, Chumak VV, Drozdovitch V, Gapanovich V, Golovanov I, Hubert P, Illichev SV, Khait SE, Kryuchkov VP, Maceika E, Maksyoutov M, Mirkhaidarov AK, Polyakov S, Shchukina N, Tenet V, Tserakhovich TI, Tsykalo A, Tukov AR and Cardis E: Risk of hematological malignancies among Chernobyl liquidators. *Radiat Res* 170: 721-735, 2008.
- Luster M, Lassmann M, Freudenberg LS and Reiners C: Thyroid cancer in childhood: management strategy, including dosimetry and long-term results. *Hormones (Athens)* 6: 269-278, 2007.
- Haas RL: Low dose radiotherapy in indolent lymphomas, enough is enough. *Hematol Oncol* 27: 71-81, 2009.
- Cuttler JM and Pollock M: Can cancer be treated with low doses of radiation? *J Am Phys Surg* 8: 108-111, 2003.
- Mallick U, Harmer C and Hackshaw A: The HiLo trial: a multi-centre randomised trial of high- versus low-dose radioiodine, with or without recombinant human thyroid stimulating hormone, for remnant ablation after surgery for differentiated thyroid cancer. *Clin Oncol* 20: 325-326, 2008.
- Frasca F, Vella V, Aloisi A, Mandarinò A, Mazzon E, Vigneri R and Vigneri P: p73 tumor-suppressor activity is impaired in human thyroid cancer. *Cancer Res* 63: 5829-5837, 2003.
- Garner E and Raj K: Protective mechanisms of p53-p21-pRb proteins against DNA damage-induced cell death. *Cell Cycle* 7: 277-282, 2008.

31. Namba H, Hara T, Tukazaki T, Migita K, Ishikawa N, Ito K, Nagataki S and Yamashita S: Radiation-induced G1 arrest is selectively mediated by the p53-WAF1/Cip1 pathway in human thyroid cells. *Cancer Res* 55: 2075-2080, 1995.
32. Rosenbluth JM and Pietenpol JA: The jury is in: p73 is a tumor suppressor after all. *Genes Dev* 22: 2591-2595, 2008.
33. Levrero M, De Laurenzi V, Costanzo A, Sabatini S, Gong J, Wang JY and Melino G: The p53/p63/p73 family of transcription factors: overlapping and distinct functions. *J Cell Sci* 113: 1661-1670, 2000.
34. Soussi T and Hjortsberg L: When mutant p53 plays hide and seek: a new challenge for diagnosis and therapy? *Trends Mol Med* 15: 1-4, 2009.
35. Leong WF, Chau JF and Li B: p53 Deficiency leads to compensatory up-regulation of p16^{INK4a}. *Mol Cancer Res* 7: 354-360, 2009.
36. Yamakoshi K, Takahashi A, Hirota F, Nakayama R, Ishimaru N, Kubo Y, Mann DJ, Ohmura M, Hirao A, Saya H, Arase S, Hayashi Y, Nakao K, Matsumoto M, Ohtani N and Hara E: Real-time in vivo imaging of p16^{INK4a} reveals cross talk with p53. *J Cell Biol* 186: 393-407, 2009.
37. Stein GH, Drullinger LF, Soulard A and Dulić V: Differential roles for cyclin-dependent kinase inhibitors p21 and p16 in the mechanisms of senescence and differentiation in human fibroblasts. *Mol Cell Biol* 19: 2109-2117, 1999.
38. Abd Elmageed ZY, Gaur RL, Williams M, Abdraboh ME, Rao PN, Raj MH, Ismail FM and Ouhtit A: Characterization of coordinated immediate responses by p16^{INK4A} and p53 pathways in UVB-irradiated human skin cells. *J Invest Dermatol* 129: 175-183, 2009.
39. Short SC, Bourne S, Martindale C, Woodcock M and Jackson SP: DNA damage responses at low radiation doses. *Radiat Res* 164: 292-302, 2005.
40. McCubrey JA, Steelman LS, Abrams SL, Lee JT, Chang F, Bertrand FE, Navolanic M, Terrian DM, Franklin RA, Libra M, *et al*: Roles of the RAF/MEK/ERK and PI3K/PTEN/AKT pathways in malignant transformation and drug resistance. *Adv Enzyme Regul* 46: 249-279, 2006.
41. Antonsson B and Martinou JC: The Bcl-2 protein family. *Exp Cell Res* 256: 50-57, 2000.
42. Wang Y, Hou P, Yu H, Wang W, Ji M, Zhao S, Yan S, Sun X, Liu D, Xing M, *et al*: High prevalence and mutual exclusivity of genetic alterations in the phosphatidylinositol-3-kinase/akt pathway in thyroid tumors. *J Clin Endocrinol Metab* 92: 2387-2390, 2007.
43. Krueger SA, Joiner MC, Weinfeld M, Piasentin E and Marples B: Role of apoptosis in low-dose hyper-radiosensitivity. *Radiat Res* 167: 260-267, 2007.
44. Enns L, Bogen KT, Wizniak J, Murtha AD and Weinfeld M: Low-dose radiation hypersensitivity is associated with p53-dependent apoptosis. *Mol Cancer Res* 2: 557-566, 2004.
45. Tsai KK, Stuart J, Chuang YY, Little JB and Yuan ZM: Low-dose radiation-induced senescent stromal fibroblasts render nearby breast cancer cells radioresistant. *Radiat Res* 172: 306-313, 2009.
46. Acosta JC, O'Loughlen A, Banito A, Guijarro MV, Augert A, Raguz S, Fumagalli M, Da Costa M, Brown C, Popov N, Takatsu Y, Melamed J, d'Adda di Fagagna F, Bernard D, Hernando E and Gil J: Chemokine signaling via the CXCR2 receptor reinforces senescence. *Cell* 133: 1006-1018, 2008.
47. Orjalo AV, Bhaumik D, Gengler BK, Scott GK and Campisi J: Cell surface-bound IL-1alpha is an upstream regulator of the senescence-associated IL-6/IL-8 cytokine network. *Proc Natl Acad Sci USA* 106: 17031-17036, 2009.
48. Matsuo SE, Leoni SG, Colquhoun A and Kimura ET: Transforming growth factor-beta1 and activin A generate antiproliferative signaling in thyroid cancer cells. *J Endocrinol* 190: 141-150, 2006.
49. Coppé JP, Patil CK, Rodier F, Sun Y, Muñoz DP, Goldstein J, Nelson PS, Desprez PY and Campisi J: Senescence-associated secretory phenotypes reveal cell-nonautonomous functions of oncogenic RAS and the p53 tumor suppressor. *PLoS Biol* 6: 2853-2868, 2008.